THE ASTROPHYSICAL JOURNAL, 317:724–732, 1987 June 15

THE CORE HELIUM FLASH AND SURFACE ABUNDANCE ANOMALIES

ROBERT G. DEUPREE AND RICHARD K. WALLACE
Los Alamos National Laboratory
Received 1986 October 2; accepted 1986 December 2

ABSTRACT

Four core helium flash calculations of varying intensity have been performed. The intensity is governed by the degree of degeneracy where the explosion occurs. All four flash models mixed residue nuclear species of the core helium flash into and above the hydrogen shell. The peak temperatures for these four flash calculations are 7.4, 8.3, 9.2, and 10.2×10^8 K, the last being about the highest temperature that can be expected without disrupting the entire core. Two other calculations were performed with the recently revised $^{12}C(\alpha, \gamma)^{16}O$ rate (Caughlan *et al.*). These calculations show slightly high peak temperatures and more α processing at the expense of ^{12}C, as one intuitively expects. These two calculations also mix material across the hydrogen shell boundary.

The primary material mixed into and above the hydrogen shell in all but one case is ^{12}C. The other major products (^{20}Ne, ^{24}Mg, ^{28}Si, and ^{32}S) result from the hot α captures that occur during the flash. The order of their abundance depends on the peak temperature, with the higher atomic weight species dominating for higher temperature flashes. Other products that are generated are ^{27}Al, ^{31}P, ^{35}Cl, ^{36}Ar, and, if the hydrogen shell is penetrated at reasonably high temperature, ^{14}N.

One of the intermediate flashes provides the most mixing, with the lower temperature flashes not producing as much processed material and the highest temperature flash generating sufficient envelope expansion that the hydrogen shell is pushed so far away that it is more difficult to penetrate.

A comparison between our results and the abundances of two stars which appear to have undergone high temperature α processing is made. The comparison is reasonably good, but both stars are in a sufficiently late evolutionary stage that the abundance peculiarities cannot be unambiguously attributed to the core helium flash.

Subject headings: nucleosynthesis — stars: abundances — stars: interiors

I. INTRODUCTION

The core helium flash occurs at the tip of the giant branch in stars of $\sim 2\ M_\odot$ and less. The event is produced by the ignition of helium by the 3α process in a stellar core where the density is sufficiently high that the electrons are degenerate. The first stellar evolution calculation by Schwarzschild and Harm (1962) concluded that this would be a hydrodynamic event, but subsequent calculations with more refined physics (e.g., Harm and Schwarzschild 1964, 1966; Demarque and Mengel 1971) found that the degeneracy could be lifted sufficiently slowly to prevent a rapid hydrodynamic explosion. A further significant step was taken by Thomas (1967, 1970), who showed that the inclusion of neutrino losses placed the location of the flash at some distance from the stellar center, rather than at the center itself. Current evolution calculations predict that the flash will occur at a mass fraction in the range 0.05–0.25 depending on the model parameters (e.g., Sweigart and Gross 1978). It is conceivable that rotation, which is not treated adequately in these models, could affect this location even further. In all these calculations peak temperatures of $\sim 2.5 \times 10^8$ K with the corresponding peak energy generation rates of 10^{13} ergs g s^{-1} were obtained.

These early calculations show what a crucial role convection plays as the peak of the core helium flash approaches. As the nuclear energy generation builds up due to local heating, neither radiation nor electron conduction can transport the energy generated very quickly. This localized heating thus leads to superadiabatic gradients and convection is initiated. Therefore, convection becomes the primary energy-loss mechanism from the flash location before the degeneracy is lifted, and it is the competition between the thermonuclear energy generation and the energy losses due to convective energy transport that determine the time scale of the temperature (and hence energy) growth. All stellar evolution calculations and two of the four one-dimensional hydrodynamic simulations (Zimmermann 1970; Villere 1976) have implicitly assumed that the convective losses dominate by forcing the convective structure to adjust instantaneously to the thermonuclear energy generation. The results obtained are consistent with this assumption, but this does not, as has sometimes been alleged, constitute proof of the validity of the assumption.

The recognition of convection as the primary energy-loss mechanism prior to the peak of the flash has led to two one-dimensional hydrodynamic calculations in which the assumption of instantaneous adjustment of convection to the thermonuclear energy generation was relaxed to an assumption in which the convective velocity in a standard mixing length treatment was allowed to lag the thermonuclear energy generation according to a certain prescription. The calculations for both a central (Edwards 1969) and noncentral (Wickett 1977) flash showed that the core should be completely disrupted, a contradiction to observations. This contradiction has also been cited as support for the instantaneous adjustment assumption, but it actually only shows that the velocity lag approach is incorrect.

These considerations led Cole and Deupree (1980, 1981) to approach the problem in a different manner. They solved the time-dependent conservation laws in two spatial dimensions with standard two-dimensional finite difference techniques. With this approach, two-dimensional convective flow patterns

are automatically generated by the unbalanced buoyancy forces in the convectively unstable region produced by the thermonuclear energy generation. Furthermore, the time-dependent interaction between the convective flow (and hence the convective energy transport) and the thermonuclear energy generation is governed by the conservation laws, rather than by some arbitrary prescription. The primary limitations of these first calculations were the poor two-dimensional resolution, restriction to two-dimensions whereas convection is clearly a three-dimensional process, the proximity of the outer radial boundary of the calculation to the location of the thermonuclear runaway, and the use of an eddy viscosity to limit the turbulent cascade. All but the last of these limitations have been addressed recently by Deupree (1984*a*): the two-dimensional resolution has been vastly improved, the calculations have been fully extended to three-dimensions with no degradation of the physical model, and the outer boundary has been made progressively more remote.

The qualitative results of all these calculations are similar, although there are some quantitative differences between two- and three-dimensional results. These results show a complex interplay between convection, expansion, and the thermonuclear energy generation. One significant ingredient is the production of small nonradial temperature fluctuations by the convective flow, which are quickly and strongly amplified by the highly temperature sensitive nuclear energy generation rates. As long as convection can transport energy inward into the previously neutrino cooled inner core, the thermonuclear runaway can be contained, but once the inner core becomes sufficiently hot that this downward energy transport is no longer efficient, one of these localized regions of high temperature and high energy generation produces a short time-scale hydrodynamic explosion. Deupree (1984*b*) has also shown that this explosion can be treated as an off-center point source explosion three-dimensionally (or on the polar axis two-dimensionally). This indicates why these calculations can achieve high temperatures and not disrupt the core as the calculations of Edwards and Wickett predicted—the extra dimensions in which expansion occurs limits both the amount of material partaking in the explosion and the explosion duration in a way no one-dimensional simulation can.

The peak temperature reached during the explosion is governed by how degenerate the exploding material is when the explosion begins. Deupree (1984*b*) has explored a large range of conditions from very mild explosions, which result in final states very similar to those found in traditional stellar evolution calculations, to violent explosions which are sufficiently strong to disrupt the entire core. The relative distribution of stars among the various alternatives is a matter for stellar evolution, in which core rotation probably plays a significant role. We can only describe the results that occur for each state.

Recently, we extended the calculations to include the hydrogen shell so that we could calculate any interaction between the core flash nuclear residue and the hydrogen shell (Deupree 1986). To mix core material into and above the hydrogen shell has been the goal of several calculations (e.g., Despain 1982; Paczyński and Tremaine 1977), but the results have either been unsuccessful or have required highly artificial circumstances. We here extend our previous results to a wider variety of explosive conditions with a better quantization of the amount of material mixed.

In the next section we present the results of the hydrodynamic evolution. We focus on the amount and types of nuclear species mixed into and above the hydrogen shell in § III and discuss what surface abundance anomalies the core helium flash can (and cannot) be expected to explain in the final section.

II. HYDRODYNAMIC EVOLUTION OF THE CORE AND THE HYDROGEN SHELL

Four core helium flash calculations have been undertaken. The difference among the four cases is the intensity of the flash, which is governed by the degeneracy at the explosion location when the explosion occurs. The phenomenology of the four calculations is similar to the much weaker flash discussed by Deupree (1986). Each calculation begins as an off-center point source explosion along the polar axis in a two-dimensional finite difference grid. The explosion is forced in the appropriate radial zone at the pole by setting the temperature in this zone to be 4×10^8 K and adjusting the density (ρ_4) there to retain hydrostatic equilibrium. Deupree (1984*b*, 1986) has shown that this well mimics the full three-dimensional result that one would obtain by following a full calculation from a traditional stellar evolution structure.

The initial conditions for the four models are given in Table 1. Included are the central density at the beginning of the calculation, the interior mass at the flash location, the density (ρ_4) and the corresponding degeneracy (η_4) at the explosion location, and the maximum temperature reached during the flash ($T_{\max}$). The Cox and Giuli (1968 chap. 24) convention for the sign of the degeneracy parameter is adopted. The role of the initial degeneracy in determining the subsequent hydrodynamic behavior has been discussed in detail by Deupree (1984*b*).

The hydrodynamic evolution for all four cases is similar. The thermonuclear burning and expansion create a high-temperature, low-density bubble of processed material in approximate hydrostatic equilibrium with its surroundings. This buoyant bubble rises, pushing the material above it upward and distorting the location of the hydrogen shell. As the bubble reaches the strongly stable region just below the hydrogen shell, it begins to expand more in the horizontal direction and penetrates the shell, most effectively from the horizontal direction.

We show this evolution in Figure 1, a contour plot of the carbon abundance, which outlines the bubble location, in two-dimensional space at various times for the intermediate intensity flash case 3. The contour levels are 0.015 in carbon abundance mass fraction. Also shown is the hydrogen shell location. The other elements included in the α process network show similar contours, although the total abundance of each is much less than carbon. We note that the penetration for this case is much stronger than for the weak flash discussed by Deupree (1986), with a sizable fraction of the entire bubble here crossing the hydrogen shell boundary. The details of the

TABLE 1

CORE HELIUM FLASH CONDITIONS

Case	ρ_c[a]	$M_r/M_\odot$	ρ_4[a]	η_4	$T_{\max}$ (10^8 K)
1.....	3.5	0.041	1.155	0.0	7.4
2.....	4.0	0.046	1.349	0.19	8.3
3.....	4.5	0.052	1.538	0.37	9.2
4.....	4.9	0.057	1.689	0.50	10.2

[a] In units of 10^5 g cm^{-3}.

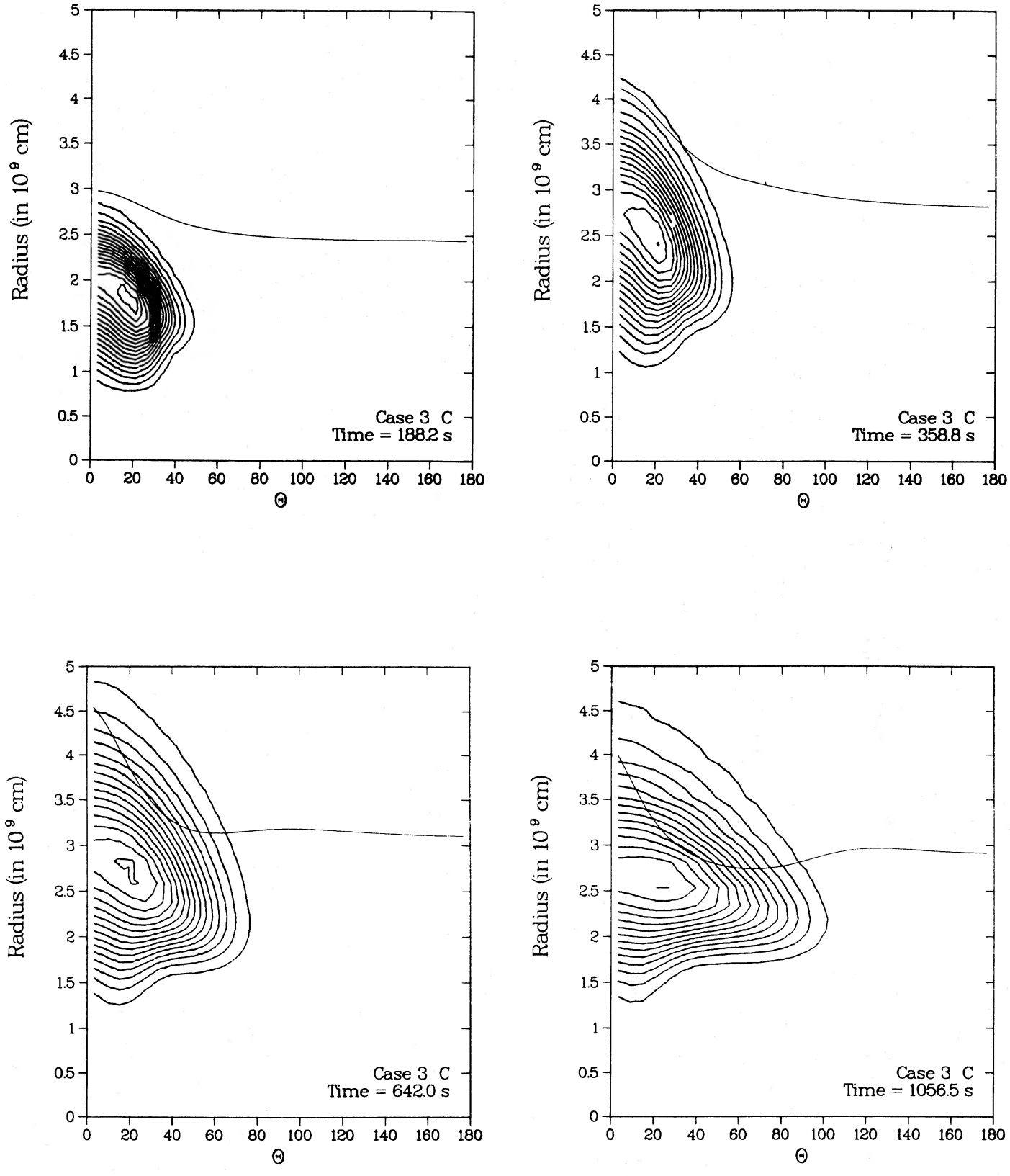

FIG. 1.—(*a*)–(*f*) Plots of the carbon abundance contours and the hydrogen shell location in two-dimensional space at various times for case 3. The contour interval of the carbon abundance is 0.015. The peak carbon abundance mass fraction in this figure is ~0.25. However, so little mass is actually partaking in the explosion that the mass fraction of all core material processed beyond helium is ~0.01. Note the strong penetration of the hydrogen shell by the carbon.

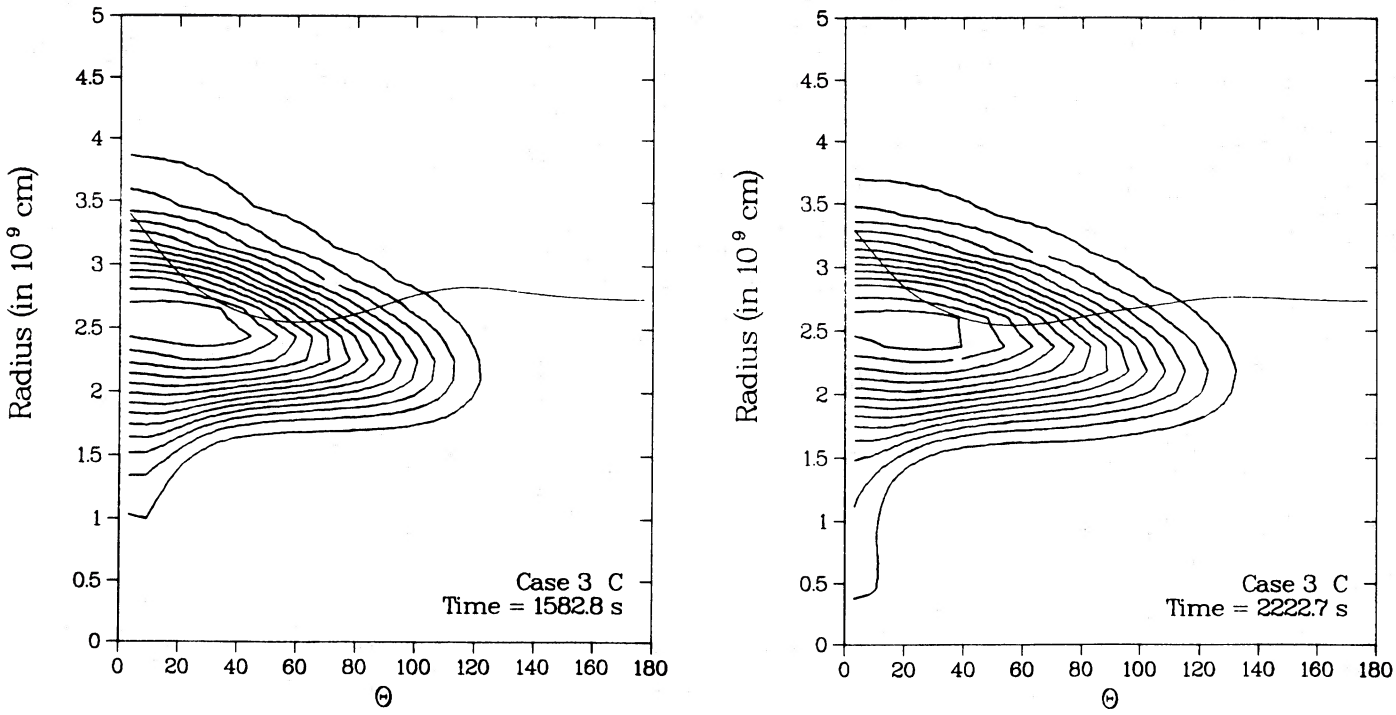

FIG. 1—*Continued*

amount of each material mixed will be discussed in the next section.

While the hydrodynamic behavior of cases 1–3 is quite similar, the most violent case 4 does show some differences. These may be seen in the time evolution of the carbon contours and the hydrogen shell location in Figure 2. Conditions appear similar to the less violent cases for about the first 350 s, but then the hydrogen shell location at $\theta = 180°$ also begins to rise (Fig. 2*b*). This is caused by the convergence at this angle of the acoustic disturbance produced by the thermonuclear explosion. This convergence finds its relief by expanding radially outward along the density gradient, resulting in the ultimate expansion of the material above the convergence point, including the hydrogen shell. This expansion of the hydrogen shell results in much less mixing than might otherwise be the case. Note that this effect would also be present in a full three-dimensional simulation. Removing the effect would require an initial nonspherical structure in addition to that produced by the explosion. Core rotation would be expected to provide such a structure, but its inclusion would require a rotation law that would be purely arbitrary at this point.

We now turn to the abundances mixed.

III. ABUNDANCES MIXED INTO AND ABOVE THE HYDROGEN SHELL

We have just shown the hydrodynamic evolution of the buoyant bubble and its penetration of the hydrogen shell. Included in the hydrodynamic simulations are the transport and mixing of the individual elements required to obtain realistic energy generation rates: ^{4}He, ^{12}C, ^{16}O, ^{20}Ne, ^{24}Mg, and ^{28}Si. The most glaring omission from the point of view of energy generation is ^{32}S, which occurs mostly in case 4 and is produced by $^{28}\mathrm{Si}(\alpha, \gamma)^{32}\mathrm{S}$.

However, there are some other elements which may be produced which could show up as abundance anomalies, even though they contribute negligibly to the energy generation. To include these elements we applied the Wallace and Woosley (1981) extensive reaction network to the density-temperature history of the bubble in the hydrodynamic simulations. We find that the other elements which may be produced in some numbers are ^{27}Al, ^{31}P, ^{32}S, ^{35}Cl, ^{36}Ar, and (in case 3 where the penetration of the hydrogen shell appears to occur at sufficiently high temperature to burn some hydrogen) ^{14}N. There may also be some other isotopes of these elements produced, but they are generally dwarfed by these more abundant isotopes.

We present the amount of each element mixed (in $10^{-5}\ M_\odot$) into or above the hydrogen shell for each of the four cases in Table 2. The values for the elements followed in the hydrodynamic simulations are taken from those calculations. The values for the other elements are computed by multiplying the amount of parent material mixed (as found in the hydrodynamics) by the ratio of the mass fractions of the trace element and its parent as found by the Wallace and Woosley

TABLE 2
ELEMENTAL ABUNDANCES MIXED INTO THE HYDROGEN SHELL ($10^{-5}\ M_\odot$)

Element	Case 1	Case 2	Case 3	Case 4
C	1.10	37.12	76.18	57.8
N	...	...	9.82	...
O	...	0.10	0.26	0.1
Ne	0.15	0.67	1.54	0.53
Na	...	...	0.0000025	...
Mg	0.011	0.50	1.12	0.52
Al	0.000031	0.00063	0.0066	0.0053
Si	0.015	0.41	4.934	2.74
P	0.0000045	0.000030	0.00084	0.0092
S	0.00042	0.015	0.986	3.10
Cl	...	...	...	0.0037
Ar	...	...	...	0.021

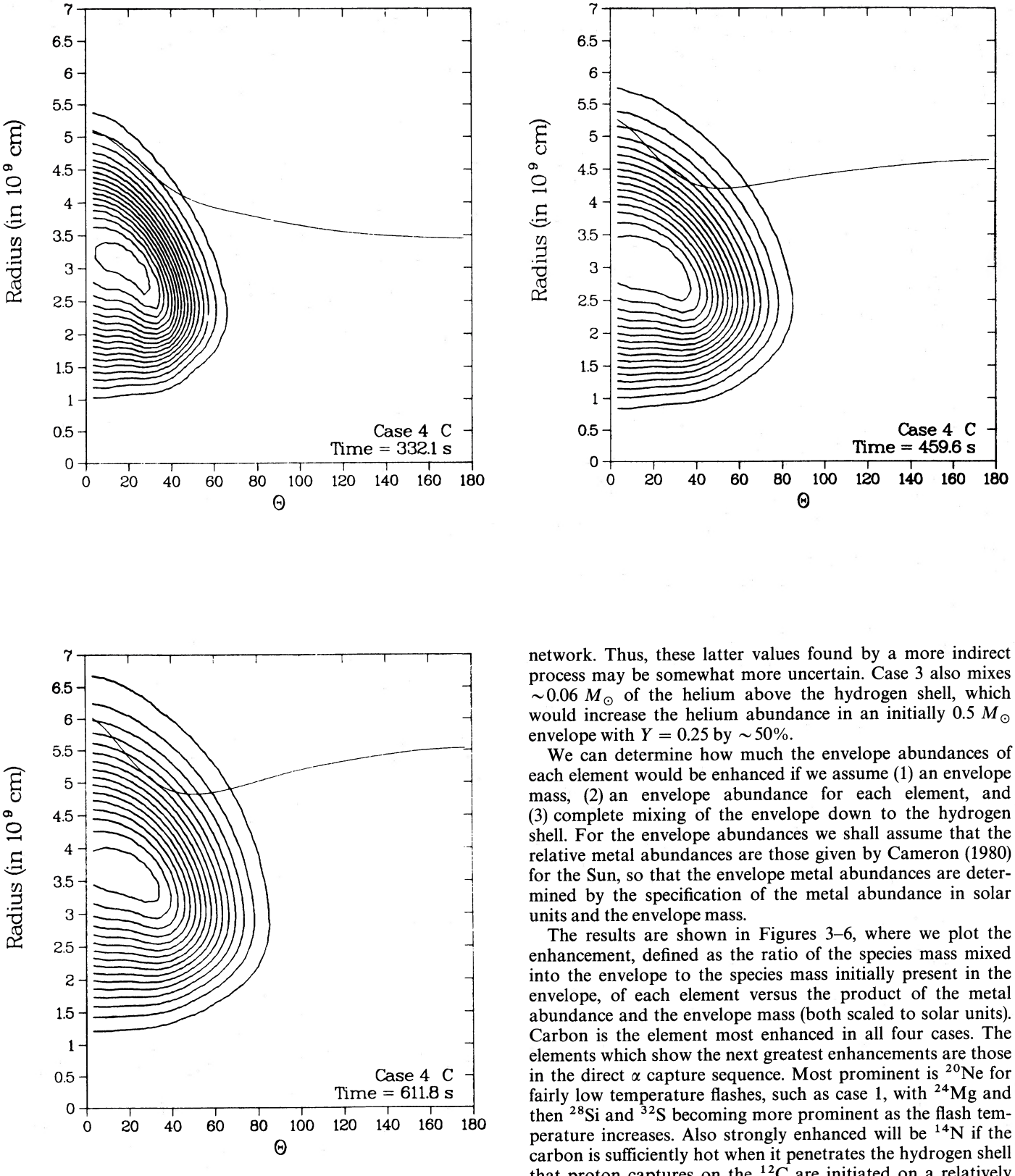

FIG. 2.—(*a*)–(*c*) Plots of the carbon abundance contours and the hydrogen shell location in two-dimensional space at various times for case 4. The carbon abundance contour interval is 0.015. Note the rise in hydrogen shell location at $\theta = 180°$, which is absent in less violent cases.

network. Thus, these latter values found by a more indirect process may be somewhat more uncertain. Case 3 also mixes $\sim 0.06\ M_\odot$ of the helium above the hydrogen shell, which would increase the helium abundance in an initially $0.5\ M_\odot$ envelope with $Y = 0.25$ by $\sim 50\%$.

We can determine how much the envelope abundances of each element would be enhanced if we assume (1) an envelope mass, (2) an envelope abundance for each element, and (3) complete mixing of the envelope down to the hydrogen shell. For the envelope abundances we shall assume that the relative metal abundances are those given by Cameron (1980) for the Sun, so that the envelope metal abundances are determined by the specification of the metal abundance in solar units and the envelope mass.

The results are shown in Figures 3–6, where we plot the enhancement, defined as the ratio of the species mass mixed into the envelope to the species mass initially present in the envelope, of each element versus the product of the metal abundance and the envelope mass (both scaled to solar units). Carbon is the element most enhanced in all four cases. The elements which show the next greatest enhancements are those in the direct α capture sequence. Most prominent is ^{20}Ne for fairly low temperature flashes, such as case 1, with ^{24}Mg and then ^{28}Si and ^{32}S becoming more prominent as the flash temperature increases. Also strongly enhanced will be ^{14}N if the carbon is sufficiently hot when it penetrates the hydrogen shell that proton captures on the ^{12}C are initiated on a relatively short (say, a few thousand second) time scale. Finally come the elements ^{27}Al, ^{31}P, ^{35}Cl, and ^{36}Ar. However, for these to be produced in any observable amount, there must be sizable enhancements of at least an appropriate member of ^{24}Mg, ^{28}Si,

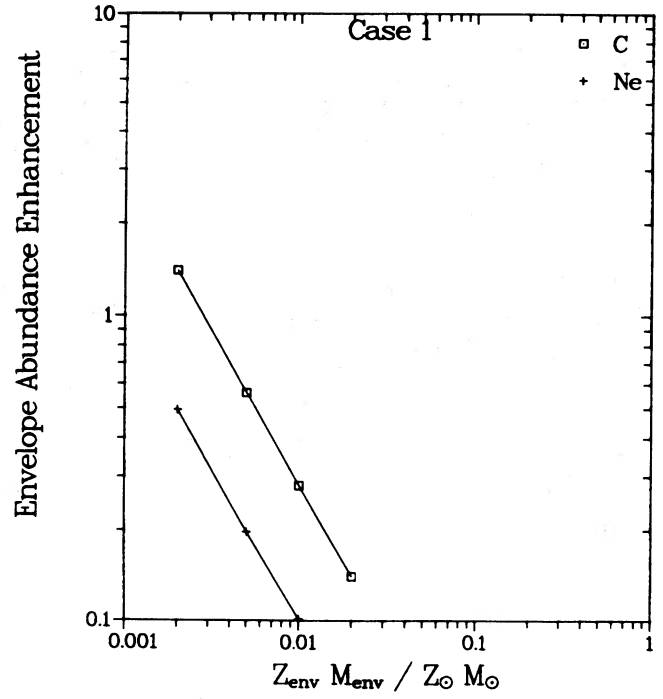

FIG. 3

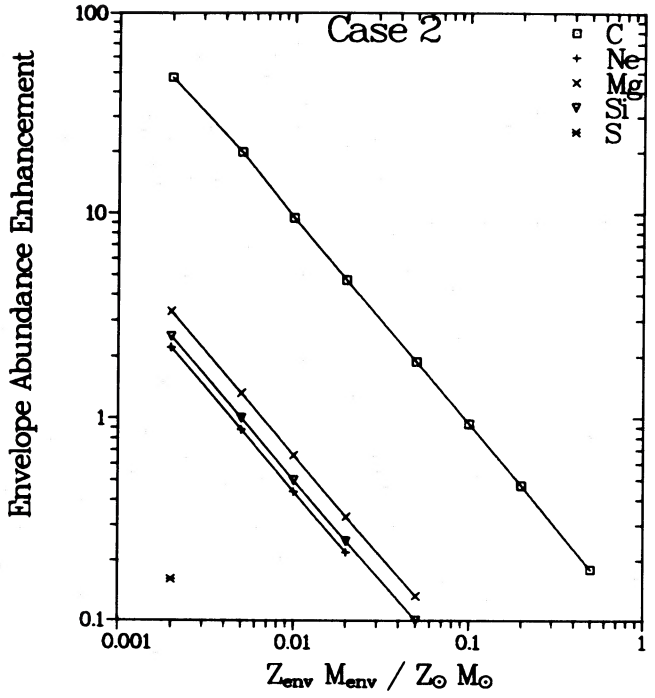

FIG. 4

FIG. 3.—Plot of the envelope abundance enhancement for various heavy elements as a function of the product of the initial envelope metal abundance and envelope mass (both in solar units) for case 1. The enhancement is defined as the ratio of the mass of a given species mixed into the envelope from the core to the mass of that species initially in the envelope. Observable enhancements of even carbon in this weak explosion would require a very metal poor, low-mass envelope.

FIG. 4.—Same as Fig. 3 for case 2. Note that it is fairly easy to obtain sizable enhancements of carbon, but other elements would only appear in very metal poor, low mass envelopes.

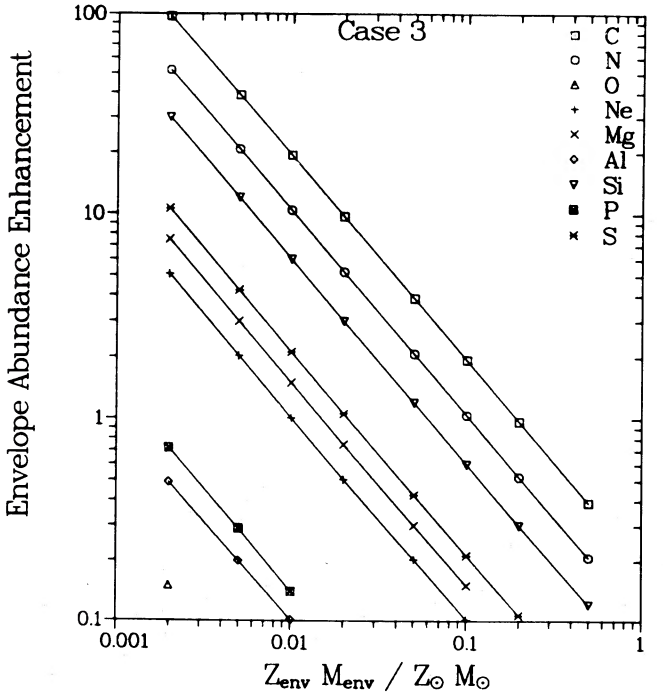

FIG. 5

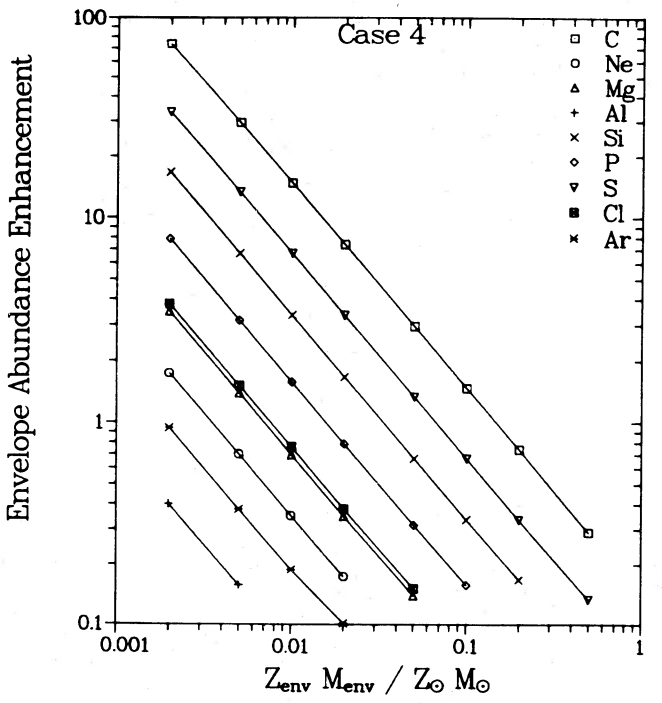

FIG. 6

FIG. 5.—Same as Fig. 3 for case 3. Note that many elements, most of them in the direct α process chain, can achieve substantial enhancements.

FIG. 6.—Same as Fig. 3 for case 4. Note the inversion of Si and S between this figure and Fig. 5, which indicates the sensitivity of the abundances to the peak temperature of the flash.

or ^{32}S. A notable exception to all of this is ^{16}O, which is effectively destroyed as soon as it is produced in all of these flashes.

From Figures 3–6 we see that, at solar abundance and reasonably large envelope masses, only ^{12}C will be enhanced to an observable extent. No enhancement will be observed in weak flashes unless both the metal abundance and envelope mass are quite low. From Figures 4–6 we see that quite an array of abundance enhancements become possible theoretically for even intermediate metal abundances and envelope masses.

Almost as significant as what is produced is what elements cannot be produced in any significant quantity. There is effectively no *s*-processing in any of these flashes (the time scales are far too short for the temperatures that occur in the flashes). Furthermore, only a trace of ^{23}Na is produced in case 2, and the amount is so small that only the most extreme envelope could expect to show any enhancement. Even then, the relative metal abundance would be so peculiar, thanks to the other elements that would have to be enhanced, that the sodium peculiarity might pass unnoticed.

The ^{12}C(α, γ)^{16}O reaction plays a fairly important role in the core helium flash because it provides a hurdle that must be passed before further α captures can occur. The energy generation rate for this reaction has recently been called into question, with a new rate given by Caughlan *et al.* (1985) being about a factor of 3 larger than the rate we used (Fowler, Caughlan, and Zimmerman 1975). We therefore recomputed cases 2 and 3 with this rate enhanced by a factor of 3 (cases 2A and 3A). The results are what one would have expected: more ^{16}O is left, although the abundance is still small, more higher Z elements are produced, the ^{12}C abundance is reduced, and the peak temperature of the flash is increased (9.0 vs. 8.3 for case 2 and 10.0 vs. 9.2 for case 3). The amount of material mixed into the envelope for cases 2A and 3A is given in Table 3 and the envelope enhancements shown in Figures 7 and 8. The dominance of ^{12}C is not so pronounced (and indeed disappears for case 3A) and the enhancements change, but the other conclusions of this section remain valid. These results also show the sensitivity of the $\eta_4 - T_{max}$ relation to the nuclear reaction rates.

We now turn to a discussion of the uncertainties of the future evolution and a comparison with observations.

TABLE 3

ELEMENTAL ABUNDANCES MIXED INTO HYDROGEN SHELL (10^{-5} $M_\odot$) FOR CASES WITH ENHANCED ^{12}C(α, γ)^{16}O RATE

Element	Case 2A	Case 3A
C	32.19	53.5
N	...	[a]
O	0.89	0.92
Ne	1.62	1.83
Na	...	...
Mg	1.42	1.85
Al	0.011	0.063
Si	4.14	10.90
P	0.00045	0.061
S	0.66	18.30
Cl	0.000015	0.029
Ar	0.0015	0.41

[a] The bubble-hydrogen shell interface has a temperature of $\sim 6 \times 10^7$, which will produce some ^{14}N, but our calculation does not go sufficiently far in time for this to become appreciable.

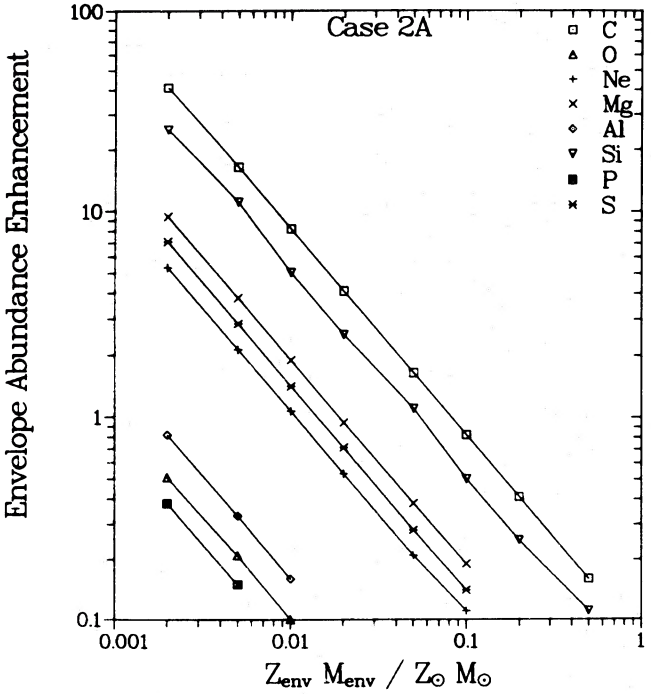

FIG. 7.—Same as Fig. 3 for case 2A, which has the same initial conditions as case 2, but with the ^{12}C(α, γ)^{16}O rate enhanced by a factor of 3. Note the similarity between case 2A and case 3, which it resembles in peak temperature.

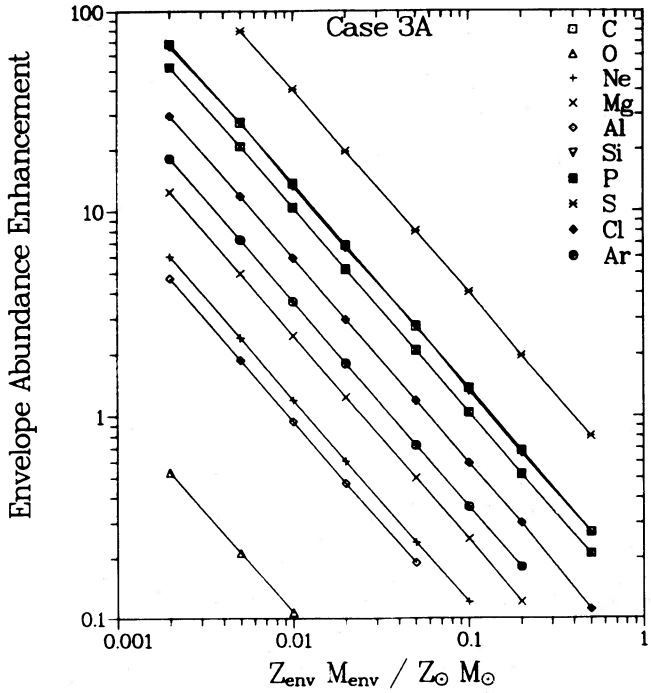

FIG. 8.—Same as Fig. 3 for case 3A, which has the same initial conditions as case 3, but with the ^{12}C(α, γ)^{16}O rate enhanced by a factor of 3. Note that increasing this reaction rate greatly enhances the higher Z elements, particularly ^{28}Si and ^{32}S, at the expense of ^{12}C.

IV. DISCUSSION

We have found that a variety of results can be obtained in core helium flash calculations depending on the degeneracy of the material at the location of the explosion. While a full suite of evolutionary calculations, preferably including the effects of convective interior heating prior to the peak of the flash (Cole, Demarque, and Deupree 1985) and a realistic approach to rotation (which does not currently exist), is required to determine the relative frequency of each type of event, one can guess that the more violent ones like cases 3 and 4 would be relatively rare because they span such a limited degeneracy range. We cannot rule out that several very weak hydrodynamic events may occur during the core flash in an individual star (most probably those with the initial temperature maximum farthest from the center). However, one violent flash sufficiently alters the core structure so as to prevent any further violent events as a part of the core helium flash. Thus, while it may be possible to mix a suitable amount of carbon (and perhaps oxygen and neon) above the hydrogen shell from a succession of weak flashes, higher Z elements require the one violent flash to occur.

One issue which clouds any discussion of the observability of any of these abundance peculiarities is the potential uncertainty in the future evolution arising from the asphericity of the hydrogen shell which is created by the rising bubble. For very mild flashes the asphericity may not affect the evolution appreciably, but it could play a role in the more violent cases, which are precisely the ones where the abundance peculiarities should stand out the most. The next evolutionary phase is certainly core helium burning, but some of the details (e.g., location on the horizontal or giant branch, helium burning lifetimes) may be murky. A further complication is the fact that some of the elements involved, such as Ne, S, and Ar, generally cannot be observed in red giants.

Nevertheless, we can make some comparisons with observed abundance anomalies. Perhaps most significant is what hydrodynamic core helium flashes by themselves do not explain. They do not produce any s-process elements, although it is conceivable that they could produce a mixing mechanism for these elements if they could be otherwise manufactured. It also seems that the core helium flash is not the source of globular cluster sodium and aluminum enhancements. These calculations do not produce sodium to the extent observed (e.g., Peterson 1980) and can produce aluminum only with an appreciable enhancement of magnesium, which is not observed (Cottrell and DaCosta 1981). Furthermore, the weak core helium flashes which do not produce enhancements of heavy elements also do not enrich the envelope helium abundance very much. Such enrichment seems to make the spectrum appear more metal rich without any metal enhancement being present (Böhm-Vitense 1979; Kamp and Deupree 1979).

The globular cluster situation where hydrodynamic core helium flashes may play a role is in explaining the complex variations in ω Cen and, to a lesser extent, in M22 (e.g., Persson *et al.*, 1980). However, this may be more of a hope than a logically derived result.

Perhaps red giant stars are not the correct objects to examine for the more violent events as represented by cases 3 and 4, since we are not sure where the evolutionary track will go in the H-R diagram (at least in terms of $T_{\rm eff}$). It may be more relevant to ask if any stars show large excesses of these α-process elements and, if so, could they have experienced hydrodynamic core helium flashes. The most interesting case in this regard is HD 46703, which Bond and Luck (1987) have found to be about one order of magnitude richer in carbon, nitrogen, oxygen, and sulfur with respect to iron than the Sun. Producing excesses of this size for carbon, nitrogen, and sulfur presents no difficulty. This would occur for a flash similar to case 4 but which penetrates the hydrogen shell at a sufficiently high temperature to process some of the carbon to nitrogen, as happens in case 3. Such an event could occur if the initial point of the explosion were closer to the hydrogen shell. The only difficulty is oxygen, which is rapidly destroyed by α captures at the temperatures of these flashes. Three possible ways to remove the difficulty are (1) a second mixture of oxygen-rich material occurring at a later evolutionary phase, (2) some previous mixing of oxygen by weak core helium flashes, or (3) remaining errors in the nuclear reaction rates. As comparison between calculations with the enhanced $^{12}C(\alpha, \gamma)^{16}O$ rate to those without reveals, such errors would have to be large to increase the ^{16}O abundance by one order of magnitude.

Both HD 46703 and BD +39°4926, which may also show a sulfur excess (Kodaira, Greenstein, and Oke 1970) are probably post–AGB stars. Thus, the origin of their α capture excesses cannot be unambiguously attributed to the core helium flash. It is conceivable that helium shell flashes could produce similar hydrodynamic and thermal behavior, although the conditions are sufficiently different that calculations must be performed to verify this. It is interesting to note, however, that in neither case do traditional stellar evolution calculations obtain the high temperatures required to produce the amount of these elements observed.

One star whose abundances can be explained entirely by a violent core helium flash is BD +10°2179. Heber (1983) has determined that, compared to the Sun, carbon and magnesium are overabundant; nitrogen, aluminum, silicon, phosphorous, and sulfur are normal; and oxygen and the higher Z than sulfur elements are underabundant. Over- and underabundances are defined as being at least a factor of 3 different from solar. These conditions could be explained by a core helium flash between cases 1 and 2 in intensity with an initial envelope metal abundance between one-third and one-tenth solar (based on the observed iron peak abundances). This could produce pronounced excesses of carbon and magnesium and sufficient enhancements of the elements between magnesium and sulfur to make them appear normal. Nitrogen could appear solar because of the enhancement produced by previous hydrogen burning, while the other elements would appear underabundant because they have not been enhanced by the flash.

The results for these two stars offer reasonably strong evidence that fairly high temperature α processing occurs. The primogenitors of both of these objects appear to be low-mass stars, for which the most likely times of high-temperature α processing would be the core helium flash and helium shell flashes. A first step in attempting to discriminate between these two would be to see if helium shell flashes are hydrodynamic events similar to helium core flashes.

Notable advances in learning more about the evolution after violent core helium flashes will be difficult. The object clearly has some multidimensional features which will not easily model in the traditional one-dimensional stellar evolution code. Furthermore, the sensitivity of the degree of violence on the details of the core structure may mean that one can no longer conscientiously neglect what are generally regarded as

second-order effects, such as rotation. This may also cloud the future evolution, since one result of the mixing during core helium flashes will be some redistribution of the core angular momentum into the outer layers. This may be relevant to the higher than expected rotational velocities found in horizontal branch stars (Peterson 1983). Whiles the inclusion of multidimensional features requires a giant step in the way we model stellar evolution, such a step may be necessary if we are to understand many of the interesting peculiar stars observed.

This work is supported by the United States Department of Energy. It is a pleasure to thank L. D. Cloutman, P. W. Cole, and C. A. Pilachowski for interesting discussions and H. E. Bond and R. E. Luck for communicating their work prior to publication. We are also grateful to the Department of Astronomy of the University of Toronto for a week's hospitality where some of these issues were examined.

REFERENCES

Böhm-Vitense, E. 1979, *Ap. J.*, **278**, 610.
Bond, H. E., and Luck, R. E. 1987, *Ap. J.*, **312**, 203.
Cameron, A. G. W. 1980, in *Nuclear Astrophysics*, ed. C. A. Barnes, D. D. Clayton, and D. N. Schramm (Cambridge: Cambridge University Press), p. 23.
Caughlan, G. R., Fowler, W. A., Harris, M. J., and Zimmerman, B. A. 1985, *Atomic Data Nucl. Data Tables*, **32**, 197.
Cole, P. W., Demarque, P., and Deupree, R. G. 1985, *Ap. J.*, **291**, 291.
Cole, P. W., and Deupree, R. G. 1980, *Ap. J.*, **239**, 284.
———. 1981, *Ap. J.*, **247**, 607.
Cottrell, P. L., and DaCosta, G. S. 1981, *Ap. J. (Letters)*, **245**, L79.
Cox, J. P., and Giuli, R. T. 1968, *Principles of Stellar Structure* (New York: Gordon and Breach).
Demarque, P., and Mengel, J. G. 1971, *Ap. J.*, **164**, 317.
Despain, K. H. 1982, *Ap. J.*, **253**, 811.
Deupree, R. G. 1984*a*, *Ap. J.*, **282**, 274.
———. 1984*b*, *Ap. J.*, **287**, 268.
———. 1986, *Ap. J.*, **303**, 649.
Edwards, A. C. 1969, *M.N.R.A.S.*, **146**, 145.
Fowler, W. A., Caughlan, G. R., and Zimmerman, B. A. 1975, *Ann. Rev. Astr. Ap.*, **12**, 215.
Harm, R., and Schwarzschild, M. 1964, *Ap. J.*, **139**, 594.
———. 1966, *Ap. J.*, **145**, 496.
Heber, U. 1983, *Astr. Ap.*, **118**, 39.
Kamp, L. W., and Deupree, R. G. 1979, *Pub. A.S.P.*, **91**, 681.
Kodaira, K., Greenstein, J. L., and Oke, J. B. 1970, *Ap. J.*, **159**, 485.
Paczyński, B., and Tremaine, S. D. 1977, *Ap. J.*, **216**, 57.
Persson, S. E., Frogel, J. A., Cohen, J. G., Aaronson, M., and Matthews, K. 1980, *Ap. J.*, **235**, 452.
Peterson, R. C. 1980, *Ap. J. (Letters)*, **237**, L87.
———. 1983, *Ap. J.*, **275**, 737.
Schwarzschild, M., and Harm, R. 1962, *Ap. J.*, **136**, 158.
Sweigart, A. V., and Gross, P. G. 1978, *Ap. J. Suppl.*, **36**, 405.
Thomas, H.-C. 1967, *Zs. Ap.*, **67**, 420.
———. 1970, *Ap. Space Sci.*, **6**, 400.
Villere, K. R. 1976, Ph.D. thesis, University of California at Santa Cruz.
Wallace, R. K., and Woosley, S. E. 1981, *Ap. J. Suppl.*, **45**, 389.
Wickett, A. J. 1977, in *Problems of Stellar Convection*, ed. E. A. Spiegel and J. P. Zahn (Berlin: Springer-Verlag), p. 284.
Zimmermann, R. E. 1970, Ph.D. thesis, University of California at Los Angeles.

ROBERT G. DEUPREE: ESS-5, MS-F665, Los Alamos National Laboratory, P.O. Box 1663, Los Alamos, NM 87545

RICHARD K. WALLACE: X-7, MS-B257, Los Alamos National Laboratory, P.O. Box 1663, Los Alamos, NM 87545